Exploring LHCb Run 3 data to search for CP violation from New Physics

D. García (Supervisor: A. Mathad)
European Organization for Nuclear Research (CERN)

August 1, 2025

Abstract

We present a summer student project in analysis of the decay channel $\bar{B} \to D^{**}\tau^-\bar{\nu}_\tau$ using LHCb Run 3 data. This study aims to explore possible signatures of CP violation arising from New Physics contributions beyond the Standard Model, particularly in processes where lepton flavor universality is tested. Due to the presence of undetected neutrinos, traditional reconstruction methods are limited; instead, we employ multivariate techniques to isolate the most probable charged pion candidates used to reconstruct D^* and D^{**} states. We also investigate angular observables and corrected mass distributions to optimize the signal extraction and prepare the ground for a full CP asymmetry measurement.

Contents

1 Introduction **2**

2 How can new physics induce CP violation? **2**

3 Summer Project **3**

3.1 Proposed Decay and Reconstruction Strategy 3
3.2 Inclusive Multivariate Isolation 4
3.3 Final selection Criteria cuts 6
3.4 Reconstruction of D^0 7
3.5 Reconstruction of D^* 7
3.6 Reconstruction of D^{**} 8
3.7 Signal and Mass corrected 8
3.8 Statistical limitations of Monte Carlo 9

4 Outlook **9**

5 Bibliography **10**

1 Introduction

Despite precise measurements from experiments like LHCb and Belle II, all observed CP violation aligns with Standard Model (SM) predictions – yet the SM allows too little CP violation to explain the matter–antimatter imbalance in the universe. This motivates the search for new sources of CP violation beyond the SM.

Recent studies of semileptonic beauty meson decays reveal deviations up to 4σ from SM expectations, particularly in decay rates involving tau vs muon leptons. These results suggest possible violations of Lepton Flavour Universality (LFU)–the principle that W bosons couple equally to all leptons.

Such anomalies have inspired new physics models, including those with leptoquarks, which could explain LFU violation and introduce additional sources of CP violation.

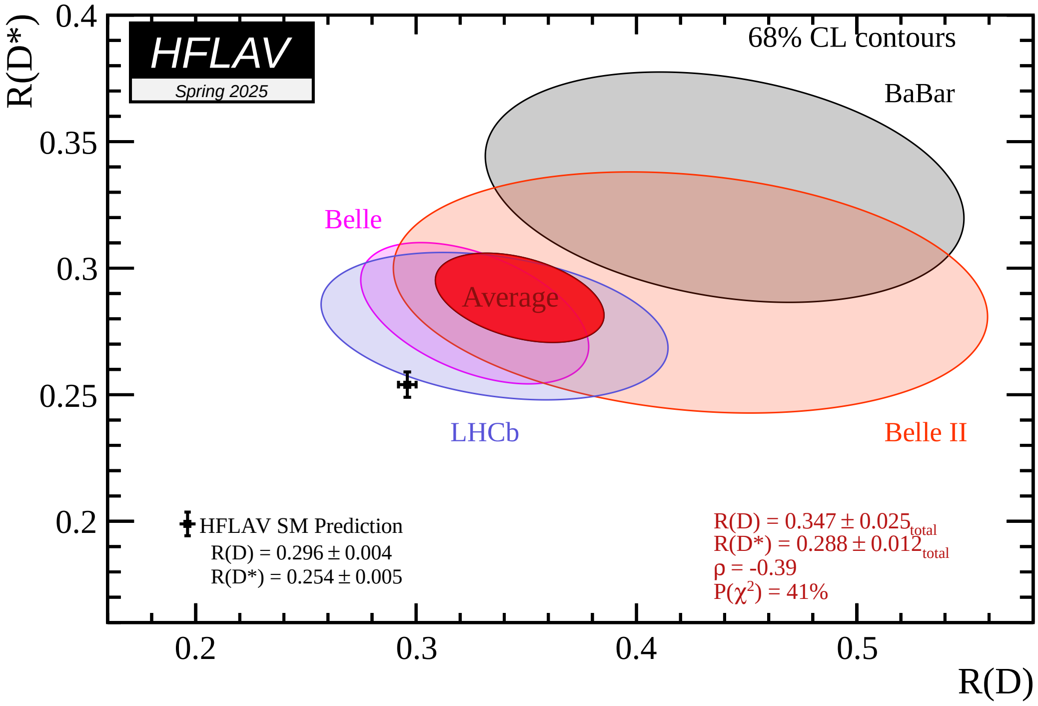

Figure 1: Comparison of the measured and predicted values of the branching ratio $R(D^*) = \frac{\mathcal{B}(B\to D^{(*)}\tau\nu)}{\mathcal{B}(B\to D^{(*)}\ell\nu)}$, where ℓ denotes a light lepton (electron or muon).

Detecting direct CP asymmetries in transitions used to test lepton flavour universality (LFU) – such as $B \to D^*\ell\nu_\ell$ – is not feasible, as these processes lack the necessary strong-phase differences required to generate such asymmetries. Instead, we focus on transitions like $B \to D^{**}\ell\nu_\ell$, where D^{**} denotes a set of orbitally excited charm states. This approach offers a clean and sensitive way to probe CP asymmetries that could only arise from physics beyond the Standard Model.

2 How can new physics induce CP violation?

A CP-violating signal requires three ingredients:

$$A_{CP} \propto |a_{\rm SM} a_{\rm NP}| \sin(\Delta\delta) \sin(\Delta\phi) \tag{1}$$

namely, non-zero SM and NP amplitudes, a strong-phase difference $\Delta\delta$, and a weak-phase difference $\Delta\phi$ from NP. The decay $\mathrm{B} \to D^{**}\tau\nu$ meets all these conditions: SM contributions are sizable, NP enters via scalar or tensor currents, strong phases arise from interference with resonances like D_1 and D_2, and weak phases stem purely from NP. These decays are thus promising probes of CP violation beyond the SM.

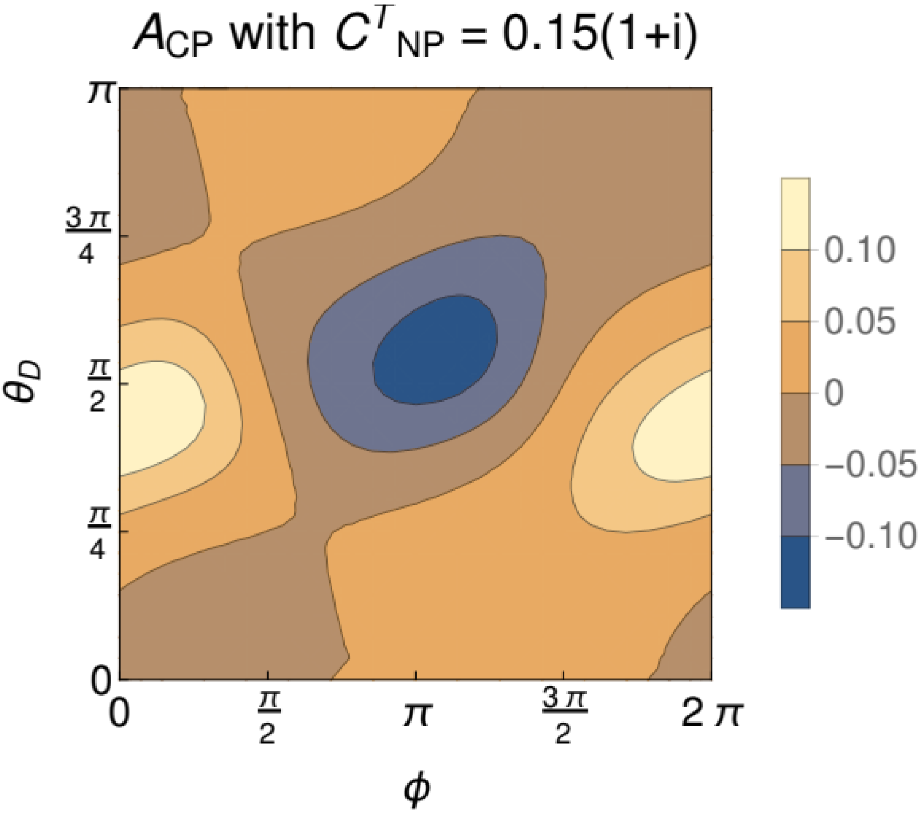

Figure 2: CP asymmetry as function of angular observables in $\mathrm{B} \to D^{**}\tau\nu$

Moreover, this method directly connects with the $R(D^*)$ puzzle, enables discrimination among various new physics scenarios, and provides a robust test of HQET and form factors in excited charm states.

3 Summer Project

3.1 Proposed Decay and Reconstruction Strategy

Decay topology. We target the semileptonic decay chain:

$$\mathrm{B}^+ \to D^{**0}\,(\to D^{*-}\,\pi^+_*)\,\tau^+(\to \mu^+\,\nu_\mu\,\bar{\nu}_\tau)$$

with subsequent decays $D^{*-} \to D^0\,\pi^-$ and $D^0 \to K^-\,\pi^+$. This channel provides sensitivity to CP-violating phases in the presence of new physics, particularly due to the interference between excited charm resonances in the D^{**0} system.

Muon trigger and neutrino challenge. By selecting the muonic decay mode of the τ lepton ($\mathcal{B} \sim 17\%$[1]), we benefit from a high trigger efficiency via the muon system. However, the presence of two undetected neutrinos (ν_τ and $\bar{\nu}_\mu$) significantly complicates the event reconstruction, rendering full invariant mass and momentum reconstruction of the B^+ meson infeasible. This missing energy manifests as a smeared B mass and broadens the kinematic distributions of interest.

Reconstruction via inclusive charged isolation. To overcome the lack of full kinematic information, we employed **Charged MVA Isolation** techniques to statistically select the optimal charged pion candidates π^- and π^+_*, critical to reconstructing intermediate states D^* and D^{**}, respectively. This approach prioritizes candidates based on their isolation from other charged tracks, topological proximity to known decay vertices, and compatibility with the decay hypothesis. The selection is reinforced by strict quality cuts on impact parameter, ghost probability, particle identification (PID), and transverse momenta, as detailed in Table 1.

3.2 Inclusive Multivariate Isolation

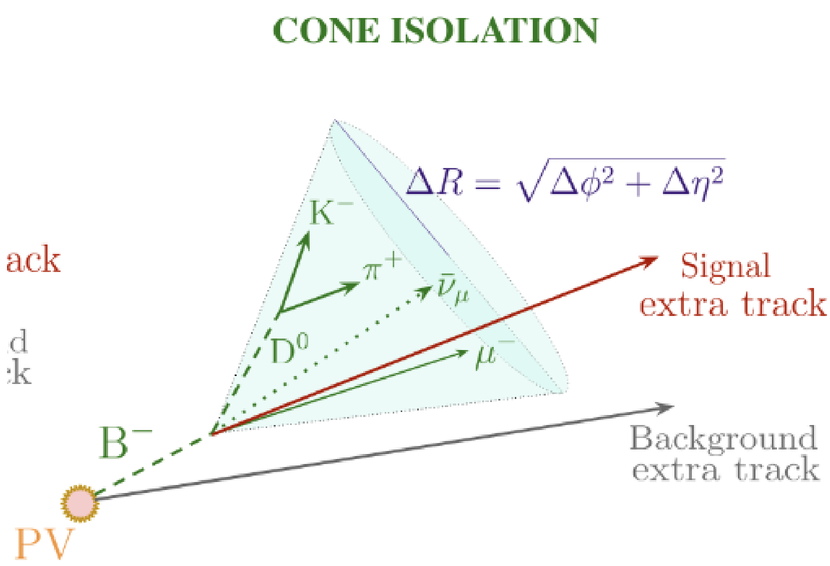

Figure 1: Analysis excluding neutrino information

Motivation and approach. Given the missing neutrinos, we cannot apply straightforward invariant mass or missing energy cuts. Instead, we use **inclusive multivariate isolation** strategies that rely solely on observed charged particles. A Boosted Decision Tree (BDT) classifier was trained to discriminate signal-like topologies from generic backgrounds, using the following observables:

- Scalar sum of track p_T within $\Delta R < 0.5$ around the muon (activity cone).
- Impact parameter significance for non-signal tracks.

[1]PDG 2024, *Review of Particle Physics*

- Flight distance significance of the reconstructed D^{**0} candidate.
- Multiplicity and geometry of secondary vertices.

This method allows us to recover discriminating power in the absence of full kinematics, by exploiting the collective behavior of the decay products.

Isolation of the soft pion π_*^+. The pion from $D^{**0} \to D^{*-}\pi_*^+$ has low to moderate p_T and aligns closely with the B^+ flight direction. Its identification is crucial for resolving the resonance structure of the D^{**0} system. We enhanced its selection through:

- Maximum p_T of tracks in a cone $\Delta R < 0.3$ around the candidate.
- Number of tracks with small longitudinal impact (Δz) relative to the D^* vertex.

These criteria suppress background from uncorrelated pions and favor the true decay chain topology, allowing for a clean reconstruction of D^{**0} despite the incomplete event information.

Selection criteria and validation. The final set of selection cuts (see Table 1) was optimized to balance signal retention with background rejection. The reconstruction of the full decay chain was validated through invariant mass windows for intermediate states, transverse momentum thresholds, and angular correlation variables ($\Delta\phi$, $\Delta\eta$) between decay products. This framework compensates for the inability to directly reconstruct the B meson and maintains high signal purity.

3.3 Final selection Criteria cuts

Table 1: Final selection Criteria cuts

Final selection criteria cuts are necessary to focus the physics analysis specifically on the event we aim to study.

Particle	Selection
μ^+	$\chi^2_{IP}(PV) > 9.0$ $P(\text{ghost}) > 0.5$ $PID\ \mu > -200$ $p > 2\text{GeV}$ `isMuon`
π^+	$\chi^2_{\text{IP}}(PV) > 9.0$ $P(\text{ghost}) < 0.5$ PID K < 2.0 $p > 2.$ GeV $p_T > 300.$ MeV
K^-	$\chi^2_{\text{IP}}(PV) > 9.0$ $P(\text{ghost}) < 0.5$ PIDK > 4.0 $p > 2.$ GeV $p_T > 300.$ MeV
D^0	$1784.8 < m < 1944.8$ MeV $p_T > 2500$ MeV $p_T(\pi) + p_T(K) > 2500$ MeV
B	$m < 10.$ GeV $\chi^2_{vtx}/\text{DOF} < 6.0$
π^-	$p > 2$ GeV `track` $\chi^2/\text{DOF} < 3$ `ISLONG` & !`ISMUON`
D^*	$1960.1 < M < 2060.1$ MeV $p_T > 1250$ MeV $\Delta m < 160$ MeV $\Delta\phi(D^0, \pi^-) < 0.1$ $\Delta\eta(D^0, \pi^-) < 0.1$

π^+_*	$p > 2$ GeV
	`ISLONG`
	`!ISMUON`

D^{**}	$\Delta\phi(D^{*-}, \pi^+_*) < 2$ $\Delta\eta(D^{*-}, \pi^+_*) < 1$
B^+	$\Delta\phi(B^+, \pi^+_*) < 2$ $\Delta\eta(B^+, \pi^+_*) < 1$

3.4 Reconstruction of D^0

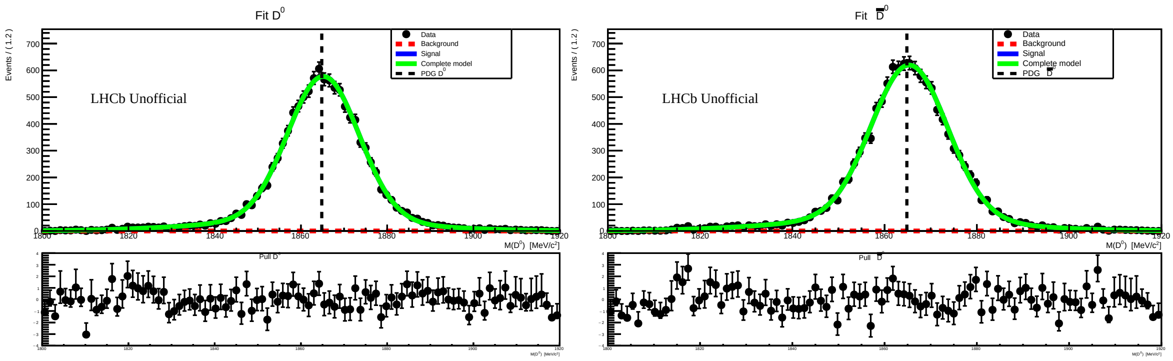

Figure 2: Double Gaussian fit of D^0 and $\bar{D}^0$ candidates showing signal extraction from invariant mass spectrum.

Table 2: Fit parameters for D^0 and $\bar{D}^0$

Particle	Gaussian Component	Fit Parameters
D^0	$\mu_1,\ \sigma_1$	$1865.2 \pm 0.1,\ 8.2 \pm 0.1$
	$\mu_2,\ \sigma_2$	$1860.9 \pm 0.7,\ 23.0 \pm 0.8$
$\bar{D}^0$	$\mu_1,\ \sigma_1$	$1865.4 \pm 0.1,\ 8.3 \pm 0.1$
	$\mu_2,\ \sigma_2$	$1861.0 \pm 0.6,\ 22.4 \pm 0.7$

3.5 Reconstruction of D^*

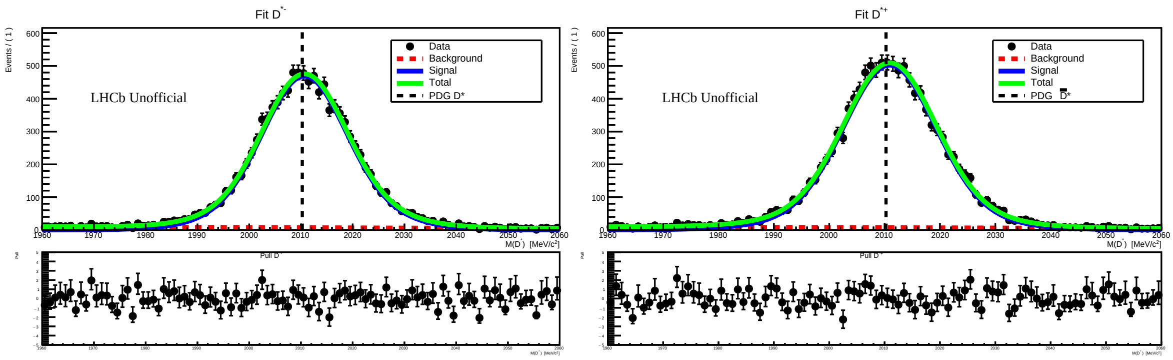

Figure 3: Double Gaussian fit of D^* and $\bar{D}^*$ meson candidates from mass spectrum analysis.

Table 3: Fit parameters for D^* and $\bar{D}^*$

Particle	Gaussian Component	Fit Parameters
D^*	$\mu_1,\ \sigma_1$	$2011.0 \pm 0.1,\ 8.1 \pm 0.3$
	$\mu_2,\ \sigma_2$	$2010.6 \pm 0.8,\ 14 \pm 2$
$\bar{D}^*$	$\mu_1,\ \sigma_1$	$2010.6 \pm 0.2,\ 7.8 \pm 0.4$
	$\mu_2,\ \sigma_2$	$2011.2 \pm 0.5,\ 13 \pm 1$

3.6 Reconstruction of D^{**}

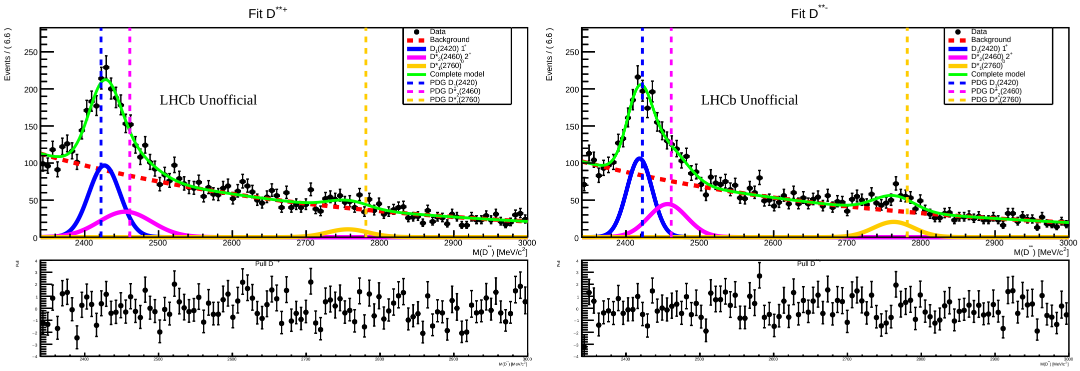

Figure 4: Mass spectrum fit of D^{**+} and D^{**-} showing contributions from various excited states: $D_1(2420)$, $D_2^*(2460)$, and $D_1^*(2760)^0$.

Table 4: Fit parameters of D^{**} excited states

Charge	**State**	**Mass** $[\mu]$	**Width** $[\sigma]$
D^{**+}	$D_1(2420)\ 1^+$	2427 ± 6	21 ± 6
	$D_2^*(2460)\ 2^+$	2455 ± 28	33 ± 13
	$D_1^*(2760)^0$	2757 ± 9	29 ± 8
D^{**-}	$D_1(2420)\ 1^+$	2418 ± 5	17 ± 3
	$D_2^*(2460)\ 2^+$	2456 ± 44	26 ± 17
	$D_1^*(2760)^0$	2763 ± 7	27 ± 6

3.7 Signal and Mass corrected

Run3 statistics allow clear resolution of $D_1(2420)^0$ and $D_2^*(2460)^0$, along with hints of the higher $D(2780)^0$ state.

To account for the undetected neutrino, the corrected mass is used:

$$m_{\text{corr}} = \sqrt{m_{\text{vis}}^2 + p_{T,\text{vis}}^2} + p_{T,\text{vis}}$$

where m_{vis} is the visible invariant mass and $p_{T,\text{vis}}$ is the transverse visible momentum orthogonal to the B FD.

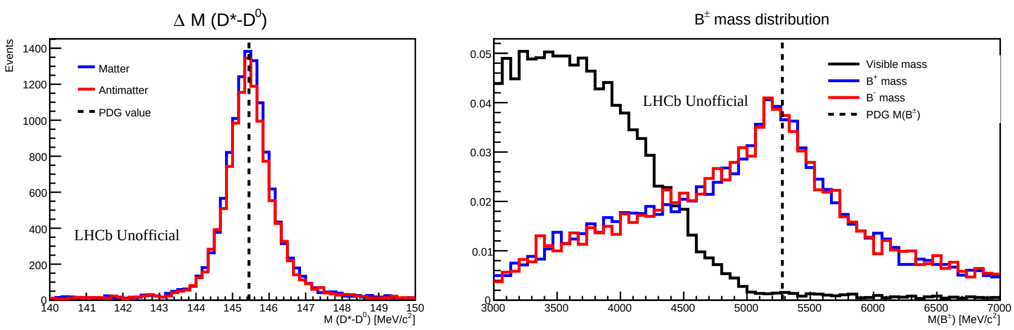

Figure 5: $\Delta M(D^* - D^0)$ and $M_{corr}(B^{\pm})$

3.8 Statistical limitations of Monte Carlo

An important part of the analysis is the reweighting of Monte Carlo data; however, when applying the same selection cuts to Monte Carlo, only 0.2% of the events survive, resulting in insufficient statistics to perform a proper analysis. Therefore, it is necessary to request Monte Carlo ntuples with sufficient statistics for the analysis.

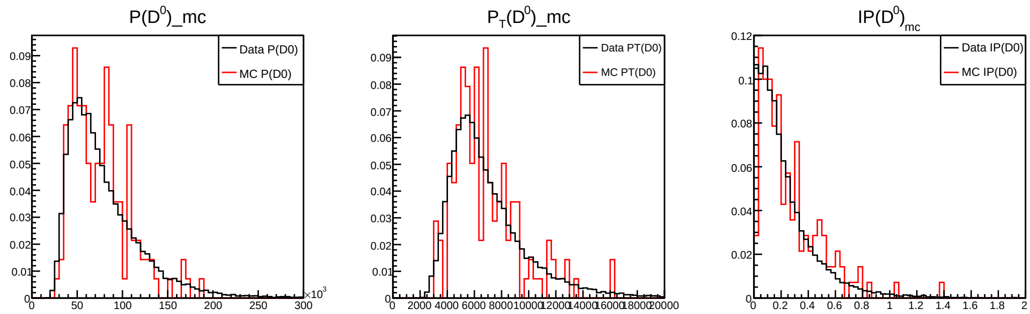

Figure 6: Comparison between data and MC in D^0

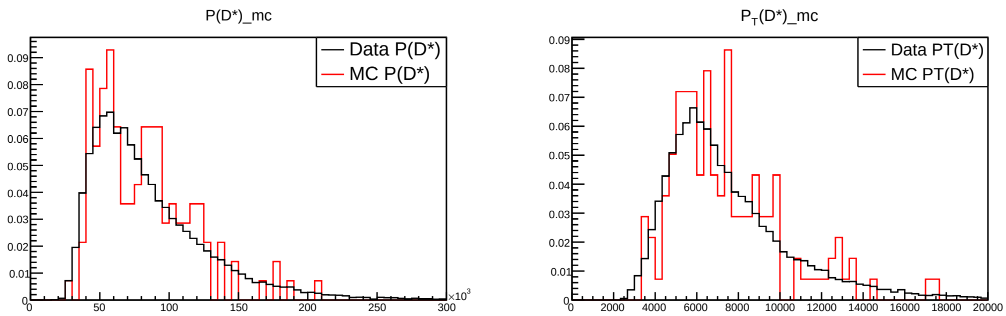

Figure 7: Comparison between data and MC in D^*

4 Outlook

With the successful reconstruction of D^{**0} resonances, the next steps involve identifying background components – such as random track combinations – and fitting the corrected mass distribution using models based on either simulation or data. This is performed in bins of the kinematic variables and separated by the decay charge to extract the raw asymmetry A_{raw}. Corrections for production and detector effects are then applied to obtain the physical CP asymmetry A_{CP}. Observing a non-zero local CP asymmetry in this analysis would be a clear indication of physics beyond the Standard Model.

Acknowledgments

Regardless of the complexity, there were people who stood by me at all times. Without my family, this would have been impossible—their support means everything to me. I am deeply grateful to my mentors and my summer project supervisor for the time they devoted. And of course, to the dear friends who, over these wonderful two months, won my heart.

5 Bibliography

1. Aloni et al., Phys. Rev. D 98, 035022 (2018). DOI
2. Bernlochner et al., Phys. Rev. D 97, 075011 (2018). DOI
3. LHCb Collab., TDR Upgrade, CERN-LHCC-2014-016. URL
4. CERN (2022), Run 3 schedule. URL